

Design of customized coated dental implants using finite element analysis

Vamsi Krishna Dommeti^{B,C}, Sumit Pramanik^{E,F}, Sandipan Roy^{A,D–F}

Department of Mechanical Engineering, SRM Institute of Science and Technology, Chennai, India

A – research concept and design; B – collection and/or assembly of data; C – data analysis and interpretation;

D – writing the article; E – critical revision of the article; F – final approval of the article

Dental and Medical Problems, ISSN 1644-387X (print), ISSN 2300-9020 (online)

Dent Med Probl. 2023;60(3):385–392

Address for correspondence

Sandipan Roy

E-mail: sandipan888roy@gmail.com

Funding sources

None declared

Conflict of interest

None declared

Acknowledgements

None declared

Received on June 14, 2021

Reviewed on August 26, 2021

Accepted on September 20, 2021

Published online on March 14, 2023

Abstract

Background. Dental implants are used as a traditional technique to replace missing teeth. In the long-term evaluation of dental implants, the stability and durability of the implant–bone interface are crucial. Furthermore, the success of dental implants depends on several factors, such as osseointegration, implant geometry and surface topography.

Objectives. The aim of the study was to investigate the effects of coating materials on dental implants by altering several parameters, including the material used, the coating thickness, and different combinations of the cortical and cancellous bones.

Material and methods. The coating materials used were hydroxyapatite (HAP), monticellite (MTC) and titanium nitride (TiN). The coating thickness was varied as 50 µm, 100 µm, 150 µm, and 200 µm. Five different bone combinations were used for the proposed finite element model. An axial compressive load of 150 N was applied.

Results. The FEA showed that the HAP coating material had a significant effect on minimizing the induced stress concentration for all 5 bone combinations. However, the MTC coating material had a significant effect only on 2 bone combinations (combination 2 and combination 3). Meanwhile, the TiN coating material induced higher stress values.

Conclusions. Based on finite element analysis (FEA), it was observed that the coating thickness greatly influenced the concentration of the mechanical stress. Indeed, when the coating thickness was relatively high, the stress concentration value significantly decreased.

Keywords: bone condition, finite element analysis, dental implant, coating thickness, coating materials

Cite as

Dommeti VK, Pramanik S, Roy S. Design of customized coated dental implants using finite element analysis. *Dent Med Probl.* 2023;60(3):385–392. doi:10.17219/dmp/142447

DOI

10.17219/dmp/142447

Copyright

Copyright by Author(s)

This is an article distributed under the terms of the Creative Commons Attribution 3.0 Unported License (CC BY 3.0) (<https://creativecommons.org/licenses/by/3.0/>).

Introduction

Dental implants have become a traditional technique used for replacing missing teeth in recent decades.¹ The success of dental implants, in both the short and long term, depends upon osseointegration and other factors, such as implant geometry and surface topography.^{2,3} For their long-term success, dental implants need improved surface characteristics and biocompatible materials, which have better mechanical properties than commercially pure titanium (Ti), including alloys such as Grade 5 titanium (Ti-6Al-4V) and titanium-zirconium (Ti-Zr).⁴

There is some evidence regarding the short-term failure of implants due to biological and biomaterial-related factors as well as surface treatment.^{5–8} Other factors, such as stress shielding and implant loosening, may directly reduce the longevity of implants and necessitate frequent revision surgeries.⁹ Furthermore, corrosion can cause extensive implant fatigue, which may shorten the life of the device and lead to its failure. In this context, the most commonly used Ti as well as Ti alloys lack the stability required to prevent corrosion in the initial stages post-implantation.^{10,11} Indeed, an investigation on the functionalization of the surface at the bone–implant interface has demonstrated that corrosive bodily fluids weaken the implant surface and cause the detachment of the device from the bone. Moreover, Ti alloys with no coating may cause infection due to biofilm formation, and lead to implant failure due to stress corrosion.^{12–15}

In people with a weakened immune system, chronic disease or addiction to tobacco products, the wound-healing processes are likely to be prolonged, which may lead to infection.¹⁶ Researchers have suggested coating dental implants with a layer of antibiotics to reduce inflammation at the wound site.¹⁷ In addition, a layer of agents such as amoxicillin, cephalothin and gentamycin can be applied to the implant surface to improve cellular responses.¹⁸ Such an approach was adopted in an *in vivo* study, in which a biomaterial surface was coated with an antibiotic for a local release.¹⁹

The coating on implants plays a significant role in overcoming biocompatibility- and mechanical stress-related issues, and can withstand most biomechanical conditions. Nonetheless, improved performance has been achieved by coating metal implants with bioceramics, apatite-based coatings and ceramic/polymer composites.^{20–26}

Bone quality plays a vital role in the customization of implants. Indeed, several studies have focused on bone quality to develop implants based on patient-specific mechanical responses.^{27,28} Another important factor for determining the long-term success of dental implants is the load transferred from the implant to the surrounding bone.

Finite element analysis (FEA) is an important tool for predicting the behavior of the implant material and the bone. The finite element method (FEM) can be used to analyze several aspects of dental implant design, including the impact of implant thread design on stress distribution. Indeed, it can be used to identify parameters that

have the greatest effect on stress distribution in the surrounding bone and the implant.^{29–31}

A previous study demonstrated that the thickness and morphology of the hydroxyapatite (HAP) layer on dental implants could be optimized based on the stress values to improve implant stability.³² Another study showed that an implant with a 150-micrometer-thick HAP layer minimized the stress concentrated in the surrounding bone.³³

The main objective of this investigation was to study the influence of the coating thickness on patient-specific implants, and to optimize the coating thickness by using 3 different coating materials – HAP, monticellite (MTC) and titanium nitride (TiN).

Modeling and methods

Finite element modeling

A three-dimensional (3D) prototype of a section of the mandibular bone was designed. The prototype had a missing tooth, and the mandibular dimensions were derived from the literature.³³ The mandibular section consisted of 2 bones, including a core soft cancellous bone, which was 24.2 mm in height and had a width of 16.3 mm, and a 2-millimeter-thick hard cortical bone. A commonly used standard dental implant model (3.75 mm in diameter) (ISP-S 1338; Adin Dental Implants, Nagpur, India) and an 11.5-millimeter-long, aluminum oxide-blasted, acid-etched Ti alloy (Ti-6Al-4V) implant (Adin Dental Implants) were used for the analysis. All of the required dimensions of the implant and the abutment were extracted for modeling using a profile projector (Fig. 1). The 3D models were constructed with coatings that conformed to the exact shape of the implant. The coatings were applied at thicknesses of 50 μm , 100 μm , 150 μm , and 200 μm . Dental feldspathic porcelain was used for the crown and a cobalt-chromium (Co-Cr) alloy was used for the metal framework. The mandible was surrounded by a gum-like structure called gingiva and the implant was placed inside the mandible. The implants and the remaining components were modeled using the SOLIDWORKS® program, v. 2017

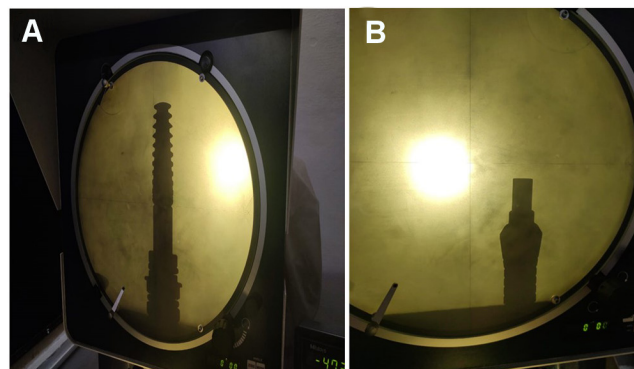


Fig. 1. Images of the dental implant (A) and of the abutment (B) in a profile projector

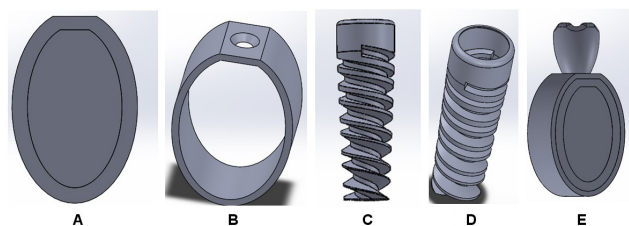


Fig. 2. Components used in the model

A – cancellous and cortical bones; B – gingiva; C – implant; D – coating layer; E – assembly of the dental implant.

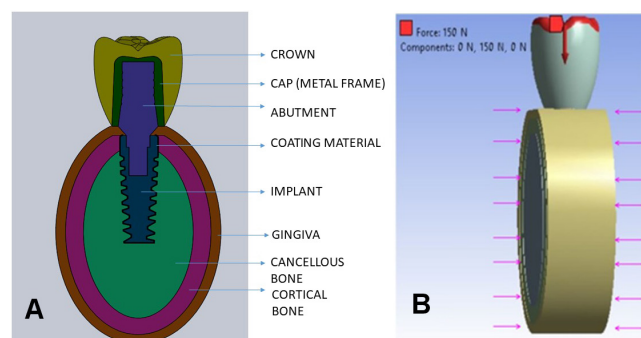


Fig. 3. Sectional view of the dental implant with the coating (A) and the dental implant with the coating at loading conditions (B): An axial compressive load of 150 N applied on the crown (the red arrow) and on both sides (from the right and from the left) of the mandibular bone section (the pink arrows)

(Dassault Systèmes, Vélizy-Villacoublay, France), and are shown in Fig. 2. The sectional view, along with loading, is shown in Fig. 3.

Finite element method

The models assembled in SOLIDWORKS were imported into the Ansys Workbench FEA tool, v. 18.2 (Ansys, Inc., Canonsburg, USA), and the file format was converted to a type that could be used for the analysis. The mesh size used throughout the modeling process was 0.2, which made it possible to obtain the convergence of the finite element model stress values; it was similar to that used by others.³⁵ The physical interactions in the contact areas of the implant–mandible section (cortical and cancellous),

implant–abutment, abutment–metal framework, and metal framework–crown interfaces during loading were taken into account using the bonded surface-to-surface contact feature in the FEA tool. The mechanical properties of the materials used for the components in the assembly are shown in Table 1.

To mimic the behavior of the bone in the mandibular section, the cortical and cancellous bones were assigned 5 different material combinations by adjusting the Young's modulus value of healthy bone by $\pm 20\%$.²⁸ The material properties of the varying combinations of the cortical and cancellous bones are shown in Table 2.²⁸

The loading conditions for the implant was an axial compressive load of 150 N applied on the crown and on both sides (from the right and from the left) of the mandibular bone section, as shown in Fig. 3B. The induced stress (the equivalent von Mises stress), transformed from the applied compressive stress through the crown to the implant, as well as 3 different coating materials – HAP,³⁶ MTC³⁷ and TiN³⁸ – at thicknesses of 50 μm , 100 μm , 150 μm , and 200 μm , were evaluated by means of FEM.

It has been observed in previous studies that the mechanical behavior of the implant depends on bone quality. However, there is still a gap in the literature regarding the effect of coated dental implants on different bone conditions.³⁹ Therefore, in the present study, implants with a varied thickness of various coating materials were investigated under static loading conditions to ascertain the optimal properties of patient-specific coated implants.

Table 2. Properties of the materials used for the cortical and cancellous bones in 5 different combinations

Combination	Young's modulus [MPa]	
	cortical bone	cancellous bone
Combination 1	13,700 (0%)	1,370 (0%)
Combination 2	10,960 (–20%)	1,096 (–20%)
Combination 3	16,440 (+20%)	1,644 (+20%)
Combination 4	16,440 (+20%)	1,096 (–20%)
Combination 5	10,960 (–20%)	1,644 (+20%)

Table 1. Properties of the materials used in the model

Component of the model	Material	Young's modulus [GPa]	Poisson's ratio	Yield strength [MPa]	Reference No.
Crown	porcelain	14	0.35	29	34
Cap (metal frame)	Co–Cr alloy	220	0.30	720	36
Abutment	surgical graded stainless steel	187.5	0.33	190	39
Implant	Ti alloy (Ti–6Al–4V)	110	0.32	800	34
Gingiva	gingiva	0.0196	0.30	–	34
HAP coating	HAP	67	0.30	–	36
MTC coating	MTC	51	0.30	–	38
TiN coating	TiN	305	0.30	–	41

HAP – hydroxyapatite; MTC – monticellite; TiN – titanium nitride; Co – cobalt; Cr – chromium; Ti – titanium.

Results

The equivalent von Mises stress values were calculated for the 3 implant coating materials under the specified loading conditions. The coating materials – HAP, MTC and TiN – were assessed at thicknesses of 50 μm , 100 μm , 150 μm , and 200 μm . The static analysis was carried out with the use of the Ansys Workbench software, v. 18.2.

Stress induced in the cortical and cancellous bones (combination 1)

Figures 4 and 5A show the distribution of the induced stress and its effect, respectively, for bone combination 1. It was observed that the von Mises stress in the cortical bone was 83.77 MPa with the HAP coating at a thickness of 50 μm . Meanwhile, in the case of the HAP coating at a thickness of 200 μm , the generated stress was reduced by 87%. On the other hand, the effect of the von Mises stress in the cancellous bone with the HAP coating at a thickness of 200 μm was reduced by 90% (Fig. 4 and Fig. 5A).

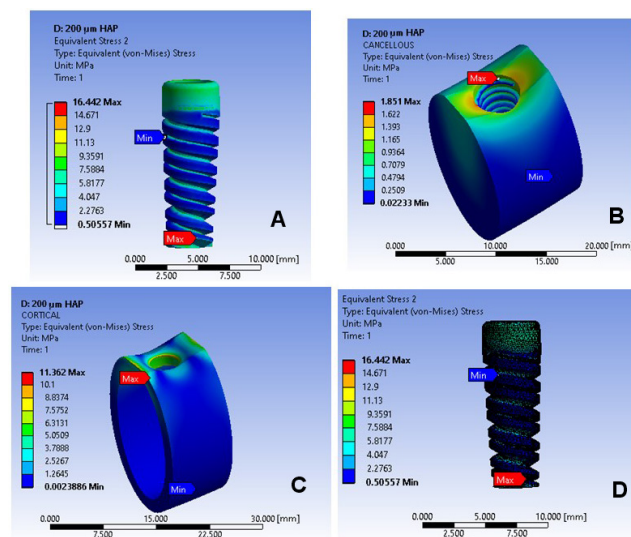


Fig. 4. Induced stress distribution for combination 1

A – stress at the coating layer (the HAP material); B – cancellous bone stress; C – cortical bone stress; D – implant stress; the arrows indicate the maximum and minimum stress at each component.

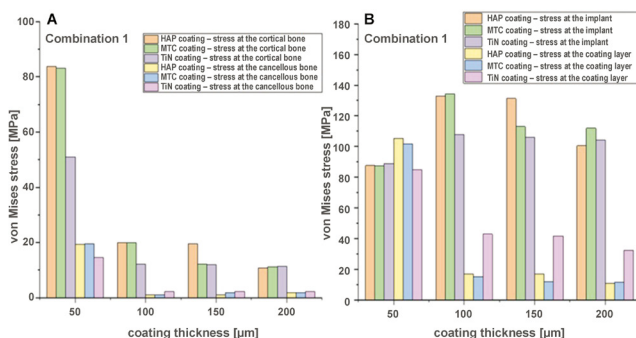


Fig. 5. Effect of the induced stress for combination 1

A – von Mises stress at the cortical and cancellous bones; B – von Mises stress at the implant and the coating layer.

Effect of stress on the implant and the coating layer (combination 1)

The stress value for the 100-micrometer HAP coating layer was 19.43 MPa, while it was reduced by nearly 90% for the 200-micrometer HAP coating layer with regard to 50 μm . The implant stress with the HAP coating was significantly different for combination 1 as compared to MTC and TiN (Fig. 5B).

Stress induced in the cortical and cancellous bones (combination 2)

Using combination 2, the maximum stress value in the cortical bone with the HAP coating at a thickness of 50 μm was over 50 MPa. In the cancellous bone, the maximum stress value with the 50-micrometer MTC coating was around 15 MPa. As the thickness of the coating increased, the stress in the cancellous bone decreased, with the 200-micrometer MTC coating reducing it by 78% (Fig. 6 and Fig. 7A).

Effect of stress on the implant and the coating layer (combination 2)

Figure 7B shows the stress values for combination 2 using coating thicknesses between 50 μm and 200 μm . The stress value for the MTC coating was reduced by 88% at a thickness of 200 μm . As the thickness of the coating layer increased, the implant stress increased as well, reaching as high as 113.81 MPa. The implant material used in this study (Ti-6Al-4V) has a yield strength ranging from 800 MPa to 950 MPa,³⁹ so the stress values were within the safe limits.

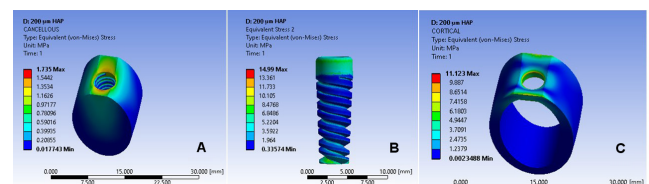


Fig. 6. Induced stress distribution for combination 2

A – cancellous bone stress; B – stress at the coating layer (the HAP material); C – cortical bone stress.

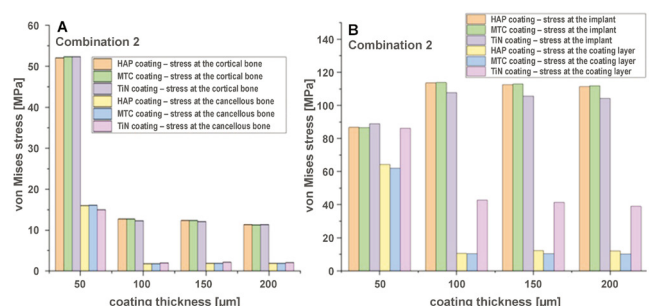


Fig. 7. Effect of the induced stress for combination 2

A – von Mises stress at the cortical and cancellous bones; B – von Mises stress at the implant and the coating layer.

Stress induced in the cortical and cancellous bones (combination 3)

For combination 3, the stress value was high at 50 μm and low at 200 μm (Fig. 8 and Fig. 9A). Using the 200-micrometer HAP coating, the stress was reduced by 87% in the cancellous bone.

Effect of stress on the implant and the coating layer (combination 3)

Figure 9B shows that as compared to the 50-micrometer coating, the stress was reduced by 81% for the 200-micrometer HAP coating, whereas there was an 83% reduction when using the 200-micrometer MTC coating. In addition, the stress at the implant was similar to that in combination 2, but was within the safe limits.

Stress induced in the cortical and cancellous bones (combination 4)

For combination 4, increasing the HAP coating thickness from 50 μm to 200 μm reduced the stress by 78% in the cortical bone. In the cancellous bone, the stress value decreased by 91% with the 200-micrometer thickness of the HAP coating as compared to the thickness of 50 μm (Fig. 10 and Fig. 11A).

Effect of stress on the implant and the coating layer (combination 4)

For the MTC coating material, the stress value was reduced by 84% for the 200-micrometer thickness as

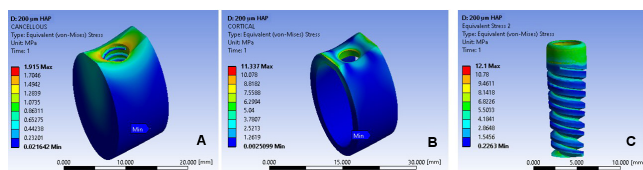


Fig. 8. Induced stress distribution for combination 3
A – cancellous bone stress; B – cortical bone stress; C – stress at the coating layer (the HAP material).

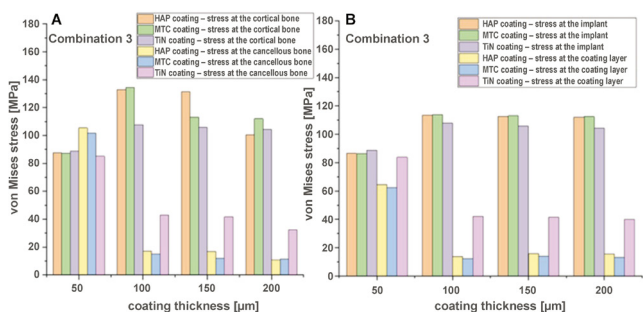


Fig. 9. Effect of the induced stress for combination 3
A – von Mises stress at the cortical and cancellous bones; B – von Mises stress at the implant and the coating layer.

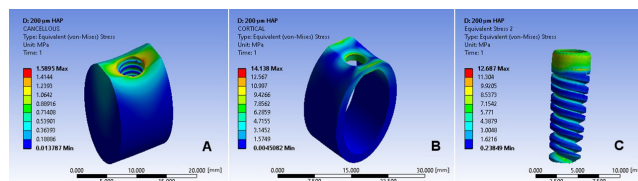


Fig. 10. Induced stress distribution for combination 4
A – cancellous bone stress; B – cortical bone stress; C – stress at the coating layer (the HAP material).

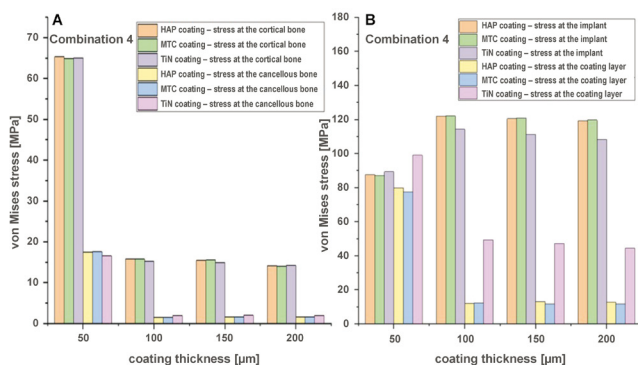


Fig. 11. Effect of the induced stress for combination 4
A – von Mises stress at the cortical and cancellous bones; B – von Mises stress at the implant and the coating layer.

compared to 50 μm . Also, the stress at the implant was 87 MPa when using the 50-micrometer coating, and 119 MPa when using the 200-micrometer coating, which was within the safe limits (Fig. 11B).

Stress induced in the cortical and cancellous bones (combination 5)

For combination 5, the stress value in the cortical bone was reduced by 77% with the 200-micrometer HAP coating as compared to the 50-micrometer coating (Fig. 12 and Fig. 13A). A similar stress reduction in the cortical bone was found for the MTC coating material, where the stress was decreased by 77% by replacing the 50-micrometer coating with a 200-micrometer layer (Fig. 13A). In addition, the stress value in the cancellous bone was reduced by 83% when using the 200-micrometer HAP coating as compared to the 50-micrometer coating (Fig. 12 and Fig. 13A).

Effect of stress on the implant and the coating layer (combination 5)

Figure 13B shows that the HAP and MTC coating materials had a more significant role in decreasing the stress than TiN. Also, the stress was reduced by 72% by increasing the coating thickness from 50 μm to 200 μm . The maximum stress value observed for the HAP-coated implant was 107.83 MPa, although this was rather low as compared to combination 2.

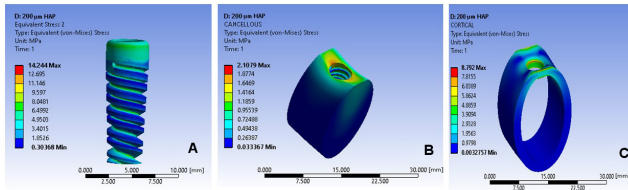


Fig. 12. Induced stress distribution for combination 5

A – stress at the coating layer (the HAP material); B – cancellous bone stress; C – cortical bone stress.

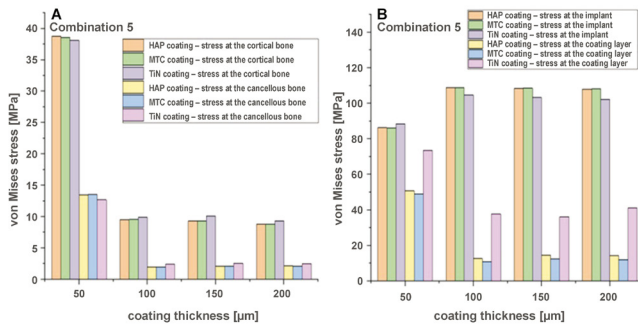


Fig. 13. Effect of the induced stress for combination 5

A – von Mises stress at the cortical and cancellous bones; B – von Mises stress at the implant and the coating layer.

Hypothesis testing

Statistical analysis was carried out on an uncoated implant model, which acted as a control. For combination 1, the mean stress value on coated implants was 87.29 MPa, while it was 89.33 MPa on uncoated implants. For combination 2, the mean stress value was 87.20 MPa on coated implants and 105.00 MPa on uncoated implants. For combination 3, the mean stress value on coated implants was 87.46 MPa and it was 76.00 MPa on uncoated implants. For combination 4, the mean stress value was 87.98 MPa on coated implants and 85.88 MPa on uncoated implants. Meanwhile, for combination 5, the mean stress value on coated implants was 86.84 MPa, and on uncoated implants, it was 84.31 MPa.

Here we accept the null hypothesis H_0 and reject the alternative hypothesis H_a . According to hypothesis testing:

$$H_0: \mu = \mu_{H0} = 1$$

The cases considered as H_a are as follows:

$H_a: \mu \neq \mu_{H0}$ The alternative hypothesis is that the population mean is not 1.

$H_a: \mu < \mu_{H0}$ The alternative hypothesis is that the population mean is less than 1.

$H_a: \mu > \mu_{H0}$ The alternative hypothesis is that the population mean is more than 1.

All the values obtained for the coatings ranged between 87 MPa and 88 MPa. Therefore, the difference is 1, which is a minimum value for variations. However, the values for uncoated implants ranged from 76 MPa to 105 MPa. Therefore, the difference in values is not equal to 1. Thus, the null hypothesis value is considered to be 1, and we accept H_0 and reject H_a . The decision chart is shown in Table 3.

Table 3. Decision-making process as to the hypotheses tested

Hypothesis	Decision	
	Accept	Reject
H_0 (true)	correct decision	error
H_0 (false)	error	correct decision

Discussion

The role of the coating on dental implants is to enhance osteoconduction, to fill gaps, and to create a bond between the bone and the implant. The selection of the coating material depends on various parameters, such as non-toxicity, corrosion resistance, fatigue strength, and durability. Hydroapatite bioceramic coatings have an additional advantage, as they reduce the healing time and have improved fixation strength.³⁹ The HAP coating thickness on dental implants ranges from 0 μm to 150 μm , and increasing the coating thickness reduces the induced stress and stress concentration.³³ Monticellite is a bioceramic that can form bone-like structures similar to the cortical bone,^{40,41} while TiN coatings have a good load-carrying capacity.⁴² For the above reasons, these 3 materials were selected as coatings in this modeling study, and were applied at thicknesses of 50 μm , 100 μm , 150 μm , and 200 μm , which is beyond those used previously (150 μm). In the present study, it was found that the optimum change in the induced stress was obtained between a coating thickness of 150 μm and 200 μm . Changing the thickness of any of the coating materials used from 150 μm to 200 μm had a significant impact, as the induced stress values were much lower as compared to coating thicknesses below 150 μm .

Bone quality is one of the parameters that affect stress distribution in the cortical and cancellous bones.⁴³ Furthermore, there is a high stress concentration in the area between the cortical and cancellous bones, as stated previously.⁴⁴ In the present work, a high stress concentration was observed at the neck area of the uncoated implant, which was reduced by coating the implant with a 200-micrometer layer. Figure 14 shows stress distribution for different bone

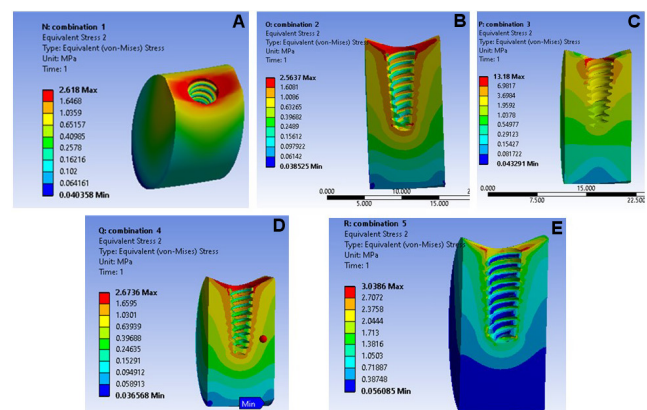


Fig. 14. Induced stress distribution in the cancellous bone for combination 1 (A), combination 2 (B), combination 3 (C), combination 4 (D), and combination 5 (E)

conditions, using uncoated implants. It was found that the 200-micrometer coating thickness reduced the stress values in the cancellous bone as compared to the uncoated implant by 34.3% (combination 1), 61.8% (combination 2), 149.0% (combination 3), 51.2% (combination 4), and 36.0% (combination 5).

Another important parameter is bone remodeling, which is a process that begins during the healing period.⁴⁵ It involves an increase in bone mass and high stress during bone formation (BF), while the stress is reduced during bone resorption (BR).⁴⁶ To ensure a successful BF process, more bone mass is needed. In this study, the microstrain values for coated implants ranged from 2,000 to 2,700 for all bone combinations. In contrast, the microstrain values for uncoated implants exceeded 3,700 for all bone combinations. Therefore, coated implants provide superior bone remodeling as compared to uncoated implants.

Limitations

The current study has several limitations, including the use of homogeneous and isotropic mechanical properties for the cortical and cancellous bones, and the simplified load conditions. Future studies should consider non-linear properties, dynamic loading, fatigue analysis, and contact analysis. Using more realistic material models would enable a better estimation of the mechanical environment at the bone–implant interface.

Conclusions

It can be concluded that the implants coated with HAP at a thickness of 200 µm were relatively superior in all 5 bone combinations. At the 200-micrometer coating thickness, both HAP and MTC gave better results than TiN. The most favorable coating thickness would be in the range of 150–200 µm, since in such conditions, the induced stress values significantly decreased for the cortical bone, the cancellous bone and the coating layer in this patient-specific study. Therefore, FEA could be used to design dental implants with patient-specific coatings.

Ethics approval and consent to participate

Not applicable.


Data availability


The datasets generated and/or analyzed during the current study are available from the corresponding author on reasonable request.


Consent for publication

Not applicable.

ORCID iDs

Vamsi Krishna Dommeti  <https://orcid.org/0000-0003-0633-9825>

Sumit Pramanik  <https://orcid.org/0000-0003-0455-1582>

Sandipan Roy  <https://orcid.org/0000-0002-6888-272X>

References

- Hämmerle CH, Glauser R. Clinical evaluation of dental implant treatment. *Periodontol* 2000. 2004;34:230–239. doi:10.1046/j.0906-6713.2003.003434.x
- Albrektsson T, Brånemark PI, Hansson HA, Lindström J. Osseointegrated titanium implants. Requirements for ensuring a long-lasting, direct bone-to-implant anchorage in man. *Acta Orthop Scand*. 1981;52(2):155–170. doi:10.3109/17453678108991776
- Guarnieri R, Miccoli G, Reda R, Mazzoni A, Di Nardo D, Testarelli L. Laser microgrooved vs. machined healing abutment disconnection/reconnection: A comparative clinical, radiographical and biochemical study with split-mouth design. *Int J Implant Dent*. 2021;7(1):19. doi:10.1186/s40729-021-00301-6
- Liu X, Chen S, Tsoi JKH, Matinlinna JP. Binary titanium alloys as dental implant materials – a review. *Regen Biomater*. 2017;4(5):315–323. doi:10.1093/rb/rbx027
- Rangert B, Krogh PH, Langer B, Van Roekel N. Bending overload and implant fracture: A retrospective clinical analysis. *Int J Oral Maxillofac Implants*. 1995;10(3):326–334. PMID:7615329.
- Quirynen M, Naert I, Van Steenberghe D. Fixture design and overload influence marginal bone loss and future success in the Brånemark system. *Clin Oral Implants Res*. 1992;3(3):104–111. doi:10.1034/j.1600-0501.1992.030302.x
- El Askary AS, Meffert RM, Griffin T. Why do dental implants fail? Part I. *Implant Dent*. 1999;8(2):173–185. PMID:10635160.
- El Askary AS, Meffert RM, Griffin T. Why do dental implants fail? Part II. *Implant Dent*. 1999;8(3):265–277. doi:10.1097/00008505-199903000-00008
- Spoerke ED, Murray NG, Li H, Brinson LC, Dunand DC, Stupp SI. A bioactive titanium foam scaffold for bone repair. *Acta Biomater*. 2005;1(5):523–533. doi:10.1016/j.actbio.2005.04.005
- Chaturvedi TP. An overview of the corrosion aspect of dental implants (titanium and its alloys). *Indian J Dent Sci*. 2009;20(1):91–98. doi:10.4103/0970-9290.49068
- Noumbissi S, Scarano A, Gupta S. A literature review study on atomic ions dissolution of titanium and its alloys in implant dentistry. *Materials (Basel)*. 2019;12(3):368. doi:10.3390/ma12030368
- Manivasagam G, Mudali UK, Asokamani R, Raj B. Corrosion and microstructural aspects of titanium and its alloys as orthopaedic devices. *Corros Rev*. 2003;21(2–3):125–160. doi:10.1515/CORRREV.2003.21.2-3.125
- Richard C, Kowandy C, Landoulsi J, Geetha M, Ramasawmy H. Corrosion and wear behavior of thermally sprayed nano ceramic coatings on commercially pure titanium and Ti-13Nb-13Zr substrates. *Int J Refract Met Hard Mater*. 2010;28(1):115–123. doi:10.1016/j.jrmhm.2009.08.006
- Machado López MM, Fauré J, Espitia Cabrera MI, Contreras García ME. Structural characterization and electrochemical behavior of 45S5 bioglass coating on Ti6Al4V alloy for dental applications. *Mater Sci Eng B*. 2016;206:30–38. doi:10.1016/j.mseb.2015.09.003
- Mehdipour M, Afshar A, Mohebbi M. Electrophoretic deposition of bioactive glass coating on 316L stainless steel and electrochemical behavior study. *Appl Surf Sci*. 2012;258(24):9832–9839. doi:10.1016/j.apsusc.2012.06.038
- Gómez-de Diego R, del Rocío Mang-de la Rosa M, Romero-Pérez MJ, Cutando-Soriano A, López-Valverde-Centeno A. Indications and contraindications of dental implants in medically compromised patients: Update. *Med Oral Patol Oral Cir Bucal*. 2014;19(5):e483–e489. doi:10.4317/medoral.19565
- Salaie RN, Besinis A, Le H, Tredwin C, Handy RD. The biocompatibility of silver and nanohydroxyapatite coatings on titanium dental implants with human primary osteoblast cells. *Mater Sci Eng C*. 2020;107:110210. doi:10.1016/j.msec.2019.110210
- Aranya AK, Pushalkar S, Zhao M, LeGeros RZ, Zhang Y, Saxena D. Antibacterial and bioactive coatings on titanium implant surfaces. *J Biomed Mater Res A*. 2017;105(8):2218–2227. doi:10.1002/jbm.a.36081

19. Rahmati M, Lyngstadaas SP, Reseland JE, et al. Coating doxycycline on titanium-based implants: Two in vivo studies. *Bioact Mater.* 2020;5(4):787–797. doi:10.1016/j.bioactmat.2020.05.007
20. Khanmohammadi S, Ilkhchi MO. Effect of suspension medium on the characteristics of electrophoretically deposited bioactive glass coatings on titanium substrate. *J Non Cryst Solids.* 2019;503–504:232–242. doi:10.1016/j.jnoncrysol.2018.10.001
21. Priyadarshini B, Rama M, Chetan, Vijayalakshmi U. Bioactive coating as a surface modification technique for biocompatible metallic implants: A review. *J Asian Ceram Soc.* 2019;7(4):397–406. doi:10.1080/21870764.2019.1669861
22. Pramanik S, Agarwal AK, Rai KN, Garg A. Development of high strength hydroxyapatite by solid-state-sintering process. *Ceram Int.* 2007;33(3):419–426. doi:10.1016/j.ceramint.2005.10.025
23. Pramanik S, Agarwal AK, Rai KN. Development of high strength hydroxyapatite for hard tissue replacement. *Trends Biomater Artif Organs.* 2005;19(1):46–51.
24. Oshkour AA, Pramanik S, Mehrali M, Yau YH, Tarlochan F, Abu Osman NA. Mechanical and physical behavior of newly developed functionally graded materials and composites of stainless steel 316L with calcium silicate and hydroxyapatite. *J Mech Behav Biomed Mater.* 2015;49:321–331. doi:10.1016/j.jmbbm.2015.05.020
25. Pramanik S, Kar KK. Nanohydroxyapatite synthesized from calcium oxide and its characterization. *Int J Adv Manuf Technol.* 2013;66:1181–1189. doi:10.1007/s00170-012-4401-z
26. Abdu Aliyu AA, Abdul-Rani AM, Ginta TL, Rao TV, Selvamurugan N, Roy S. Hydroxyapatite mixed-electro discharge formation of bio-ceramic Lakargiite (CaZrO_3) on Zr-Cu-Ni-Ti-Be for orthopedic application. *Mater Manuf Process.* 2018;33(16):1734–1744. doi:10.1080/10426914.2018.1512122
27. Roy S, Dey S, Khutia N, Chowdhury AR, Datta S. Design of patient specific dental implant using FE analysis and computational intelligence techniques. *Appl Soft Comput.* 2018;65:272–279. doi:10.1016/j.asoc.2018.01.025
28. Kasani R, Sai Attili BK, Dommeti VK, Merdji A, Biswas JK, Roy S. Stress distribution of overdenture using odd number implants – a finite element study. *J Mech Behav Biomed Mater.* 2019;98:369–382. doi:10.1016/j.jmbbm.2019.06.030
29. El-Anwar MI, El-Zawahry MM, El-Mofty MS. Load transfer on dental implants and surrounding bones. *Aust J Basic Appl Sci.* 2012;6(3):551–560.
30. Jain V, Dommeti VK, Rana M, Roy S. Influences of stresses on dental implant threads using finite-element analysis. *J Long Term Eff Med Implants.* 2019;29(2):125–133. doi:10.1615/JLongTermEffMed-Implants.2019031812
31. Roy S, Panda D, Khutia N, Chowdhury AR. Pore geometry optimization of titanium (Ti6Al4V) alloy, for its application in the fabrication of customized hip implants. *Int J Biomater.* 2014;2014:313975. doi:10.1155/2014/313975
32. Baltag I, Watanabe K, Kusakari H, et al. Long-term changes of hydroxyapatite-coated dental implants. *J Biomed Mater Res A.* 2000;53(1):76–85. doi:10.1002/(sici)1097-4636(2000)53:1<76::aid-jbm11>3.0.co;2-4
33. Hedia HS. Effect of coating thickness and its material on the stress distribution for dental implants. *J Med Eng Technol.* 2007;31(4):280–287. doi:10.1080/03091900600861616
34. Kayabaşı O, Yüzbasioğlu E, Erzincanlı F. Static, dynamic and fatigue behaviors of dental implant using finite element method. *Adv Eng Softw.* 2006;37(10):649–658. doi:10.1016/j.advengsoft.2006.02.004
35. El-Abidine Arab AZ, Merdji A, Benaissa A, et al. Finite-element analysis of a lateral femoro-tibial impact on the total knee arthroplasty. *Comput Methods Programs Biomed.* 2020;192:105446. doi:10.1016/j.cmpb.2020.105446
36. Oshkour AA, Talebi H, Shirazi SF, et al. Parametric study of radial functionally graded femoral prostheses with different geometries. *Meccanica.* 2015;50:1657–1678. doi:10.1007/s11012-015-0121-4
37. Chen X, Ou J, Kang Y, et al. Synthesis and characteristics of monticellite bioactive ceramic. *J Mater Sci Mater Med.* 2008;19(3):1257–1263. doi:10.1007/s10856-007-3233-0
38. Holmberg K, Ronkainen H, Laukkanen A, Wallin K, Erdemir A, Eryilmaz O. Tribological analysis of TiN and DLC coated contacts by 3D FEM modelling and stress simulation. *Wear.* 2008;264(9–10):877–884. doi:10.1016/j.wear.2006.12.084
39. Roy S, Das M, Chakraborty P, et al. Optimal selection of dental implant for different bone conditions based on the mechanical response. *Acta Bioeng Biomech.* 2017;19(2):11–20. doi:10.5277/ABB-00530-2015-03
40. Roy S, Khutia N, Das D, et al. Understanding compressive deformation behavior of porous Ti using finite element analysis. *Mater Sci Eng C.* 2016;64:436–443. doi:10.1016/j.msec.2016.03.066
41. Lee JJ, Rouhfar L, Beirne OR. Survival of hydroxyapatite-coated implants: A meta-analytic review. *J Oral Maxillofac Surg.* 2000;58(12):1372–1379. doi:10.1053/joms.2000.18269
42. Choudhury P, Agrawal DC. Sol-gel derived hydroxyapatite coatings on titanium substrates. *Surf Coat Technol.* 2011;206(2–3):360–365. doi:10.1016/j.surfcoat.2011.07.031
43. Kitagawa T, Tanimoto Y, Nemoto K, Aida M. Influence of cortical bone quality on stress distribution in bone around dental implant. *Dent Mater.* 2005;24(2):219–224. doi:10.4012/dmj.24.219
44. Taharou B, Merdji A, Hillstrom R, et al. Biomechanical evaluation of bone quality effect on stresses at bone-implant interface: A finite element study. *J Appl Comput Mech.* 2021;7(3):1266–1275. doi:10.22055/JACM.2020.32323.2005
45. Mavrogenis AF, Dimitriou R, Parvizi J, Babis GC. Biology of implant osseointegration. *J Musculoskelet Neuronal Interact.* 2009;9(2):61–71. PMID:19516081.
46. Frost HM. Bone's mechanostat: A 2003 update. *Anat Rec A Discov Mol Cell Evol Biol.* 2003;275(2):1081–1101. doi:10.1002/ar.a.10119